RSC Advances

PAPER

View Article Online
View Journal | View Issue

Cite this: *RSC Adv.*, 2023, **13**, 25129

Electrochemical sensor based on bio-inspired molecularly imprinted polymer for sofosbuvir detection†

Mahmoud A. Soliman,[a] Amr M. Mahmoud, *[b] Eman S. Elzanfaly[bc] and Laila E. Abdel Fattah[ab]

The electropolymerized molecularly imprinted polymers (MIP) have enabled the utilization of various functional monomers with superior selective recognition of the target analyte template. Methyldopa is an attractive synthetic dopamine analogue which has phenolic, carboxylic, and aminic functional groups. In this research, methyldopa was exploited to fabricate selective MIPs, for the detection of sofosbuvir (SFB), by a simple electropolymerization step onto a disposable pencil graphite electrode (PGE) substrate. The interaction between methyldopa, as a functional monomer, and a template has been investigated experimentally by UV spectroscopy. A polymethyldopa (PMD) polymer was electrografted onto PGE in the presence of SFB as a template. X-ray photoelectron spectroscopy (XPS), electrochemical impedance spectroscopy (ESI), and cyclic voltammetry (CV) were used for the characterization of the fabricated sensor. Differential pulse voltammetry (DPV) of a ferrocyanide/ferricyanide redox probe was employed to indirectly detect the SFB binding to the MIP cavities. The sensor shows a reproducible and linear response over a dynamic linear range from 1.0×10^{-11} M to 1.0×10^{-13} M of SFB with a limit of detection of 3.1×10^{-14} M. The sensor showed high selectivity for the target drug over structurally similar and co-administered interfering drugs, and this enabled its application to detect SFB in its pharmaceutical dosage form and in spiked human plasma samples.

Received 9th June 2023
Accepted 10th August 2023

DOI: 10.1039/d3ra03870j

rsc.li/rsc-advances

Introduction

Catecholamine derived polymers, such as dopamine and its naturally present analogues, have lately been of interest in various scientific disciplines as they are known as versatile and promising functional materials in materials science, and chemical and biomedical sciences.[1,2] They are bio-inspired from the adhesive proteins in the foot of marine mussels, which are, in turn, rich in amine and catechol moieties.[3,4] Catecholamine polymers are useful because they are good adherent materials, providing an antifouling surface and biocompatibility, in addition to having long durability. This trait allows their extensive usage in surface modification and material functionalization.[5] These specific polymers have good hydrophilicity and their structure contains inherent functional groups ranging from phenolic hydroxyls (OH), imines to amines.[6] Catecholamines are usually subject to oxidation and polymerization in a spontaneous way *via* self-assembly in a medium with an alkaline pH under aerobic conditions constituting a polymeric film that is thin with a quinone-based structure.[7,8] However, the self-polymerization pathway has some disadvantages as it is incompatible with alkaline-labile substrate materials. Moreover, self-polymerization demands a high concentration of monomer in addition to a long deposition time.[1] A substitute approach for traditional polymerization is to adopt advanced approaches such as cyclic voltammetry (CV) which offers a faster and uniform deposition in slightly neutral or acidic solutions. Dopamine and L-dopa are effective functional monomers for preparing molecularly imprinted polymers (MIP) using electropolymerization with a high capability to recognize the template drug in various matrices, and have already been investigated in previous studies.[9–12] Using dopamine and L-dopa as functional monomers to prepare a copolymers have been reported as a novel approach of sensing.[13]

With the increasing prominence of MIPs, being used as intelligent adsorption particles, the scope of exploiting new functional monomers has expanded to cover new derivatized molecules with extra functional groups which can bind in a more effective way with specific templates.[14] Methyldopa, a dopamine synthetic analogue, is amenable to polymerization to form poly-methyldopa (PMD).[1,7] The PMD has recently gained

[a]*Misr University for Science and Technology, Faculty of Pharmaceutical Sciences and Drug Manufacturing, Department of Analytical Chemistry, 6th of October City, 12566, Egypt*

[b]*Cairo University, Faculty of Pharmacy, Department of Analytical Chemistry, Cairo, 12613, Egypt. E-mail: amr.bekhet@pharma.cu.edu.eg*

[c]*Pharmaceutical Analytical Chemistry Department, Faculty of Pharmacy and Drug Technology, Egyptian Chinese University, Cairo, Egypt*

† Electronic supplementary information (ESI) available. See DOI: https://doi.org/10.1039/d3ra03870j

great attention in the analytical chemistry field due to the extra carboxylic group (COOH) present in its structure. Liu *et al.* described the first use of PMD as a fluorescent sensor to monitor tyrosinase activity by mixing methyldopa and ethanolamine.[15] In addition, methyldopa self-assembly has been utilized as an anchor for metallic nanoparticles, inhibiting their easy oxidation and enhancing their surface properties as well. This modification has shown an amazing catalytic performance in aryl nitrile synthesis from the corresponding halides[16] and has been successfully applied for phenylephrine and acetaminophen determination.[17] Our group has lately used methyldopa as a novel electroactive functional monomer to prepare electropolymerized PMD for the selective detection of darifenacin.[18] Electrochemical sensors that are modified with MIPs have offered new methods of determination with high selectivity of various analytes in biological samples in addition to dosage forms.[19,20] Many strategies have been applied for MIP synthesis together with precipitation polymerization, surface imprinting, electropolymerization and bulk polymerization.[21] During the electropolymerization process, the functional monomers were polymerized while the template drug is present on the electrode surface, and then a specific voltage or current was applied.[22–24] Accordingly, the advantages of electropolymerization strategies, compared to other traditional imprinting techniques, can be defined as being highly reproducible, cost-effective, rapid, and simple without the need of UV exposure, various polymerization initiators, or long-time heating. In addition, electropolymerization leads the way for the utilization of a wide array of light-sensitive and/or heat sensitive materials as functional monomers.[1] An extra benefit of electropolymerization is that the polymeric film thickness can be controlled by adjusting different experimental variables such as scan rate or number of the voltammetric cycles, and thus forming uniform, well-adherent, and thin films.[25]

Hepatitis C virus (HCV) is known to be a harmful virus which causes lethal and horrible diseases. In the United States (US), HCV causes about 3–5 million of deaths whereas about 170 million people are infected all over the world. Severe cases of hepatitis are usually asymptomatic but once it becomes chronic, it leads to serious deadly complications such as hepatic cancer and death.[26] Options of treatment for chronic cases of hepatitis C have significantly advanced since 2011. This is due to the development and synthesis of directly acting antivirals such as SFB. Sofosbuvir isopropyl (2*S*)-2-{[(*S*)-{[(2*R*,3*R*,4*R*,5*R*)-5-(2,4-dioxo-3,4-dihydro-1(2*H*)-pyrimidinyl)-4-fluoro-3-hydroxy-4-methyltetrahydro-2-furanyl]methoxy}(phenoxy)phosphoryl] amino}propanoate. Fig. 1 shows the direct acting antiviral medication, which is a prodrug nucleotide analog. The metabolism of SFB in its active form works as a defective substrate for the non-structural protein 5B (NS5B) synthesis.[27,28] The SFB is co-administered with different antiviral drugs such as ledipasvir, daclatasvir, simeprevir, or ribavirin.[28–31] Hence, there is a great need for an ecofriendly, fast, easy, and selective procedure for the detection of SFB alone or in the presence of other antiviral drugs, which does not require a long extraction, complicated equipment or sample collection procedures, and without expensive solvents. Many analytical methods were established for SFB determination such as the most recent HPLC,[32–34] LC-MS/MS,[35–37] spectrophotometric,[26,38] and HPTLC.[39] These methods have a very high accuracy, however, the majority of them require a lot of complicated extraction procedures in addition to requiring highly expensive instrumentation and a high rate of solvent consumption.

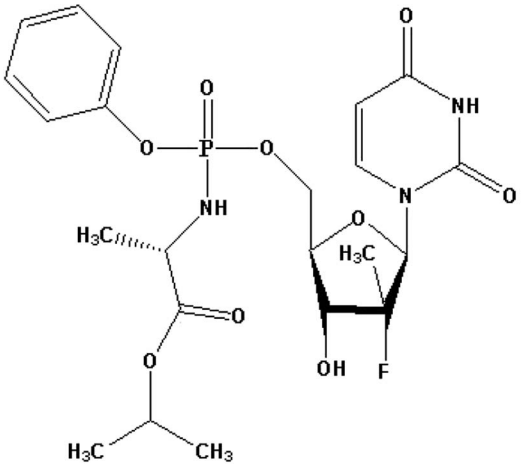

Fig. 1 The chemical structure of sofosbuvir.

The indirect method is based on the formation of 3D cavities for the selective detection of the analyte of interest. After washing, the 3D cavities are vacant, and redox probes such as ferrocyanide/ferricyanide or ferrocene carboxylic acid[40–42] can diffuse into the cavities and give an electrochemical response. Upon addition of the analyte of interest, it binds tightly into the 3D cavities and hence, the redox probe signal decreases.[43,44] The calibration curve is a correlation between the analyte concentration and the decrease of redox probe signal.[42]

Four voltammetric methods were reported recently for the purpose of determining SFB. Two of the methods were dependent on SFB direct oxidation on a glassy carbon electrode (GCE) modified surface using ionic liquid, carbon nanotubes, reduced graphene oxide (rGO), and MnO_2 (ref. 45) or cobalt nanoparticles.[46] An additional voltammetric method based on MIP was built using gold nanoparticles, *para*-aminothiophenol (PTP)–MIP,[41] and co-doped graphene quantum dots to modify a PGE substrate. There was an additional method that is similar to the previously-mentioned method which uses *ortho*-aminophenol[40] as functional monomer.

In this current work, methyldopa, as an electroactive functional monomer, was employed in the preparation of MIP films using an electropolymerization technique for constructing a new electrochemical sensor for selective recognition of SFB in pharmaceutical dosage form and samples of spiked human plasma were examined. In the beginning, the plan was to study the interaction between methyldopa as a functional monomer as well as the template SFB with UV-spectrophotometry. After that, it was planned to optimize different electrochemical parameters for the purpose of achieving the optimum conditions for the electrografting of methyldopa. Surface characterization by SEM and XPS was performed. The proposed sensor was successfully used for voltammetric measurement of SFB in

pharmaceutical dosage form and spiked human plasma samples.

Material and methods

Instruments

Electrochemical experiments were conducted on a PalmSens4 potentiostat operated with PSTrace 5.0 software (PalmSens, The Netherlands). The electrochemical operating cell consisted of a working electrode of a PGE (HB 0.9 mm diameter, Rotring, Germany), a counter electrode of platinum, and a reference electrode of Ag/AgCl. The UV-visible double beam spectrophotometer (Shimadzu EPMA-1610, Tokyo, Japan) was used for the spectrophotometric measurements. The surface chemical composition was characterized using XPS (K-Alpha X-ray photoelectron spectrometer, ThermoFisher Scientific, WI, USA).

Reagents and materials

Pure SFB was kindly donated by Eva Pharma (Cairo, Egypt). Nucleobuvir tablets (with 400 mg of SFB in each tablet) were used in a commercially available dosage form (Eva Pharma, Cairo, Egypt). Potassium chloride, methanol, glacial acetic acid, methyldopa, potassium ferricyanide ($K_3[Fe(CN)_6]$), and potassium ferrocyanide ($K_4[Fe(CN)_6]$) were obtained from Sigma-Aldrich (Darmstadt, Germany). Other reagents and chemicals were of analytical grade. Double-distilled water was obtained from a New Human Power I water purification system (Human Corporation, Seoul, South Korea). Phosphate buffer was prepared freshly, and adjusted to the required pH (6.5–7.0).

Study of the interaction between the monomer and SFB

The interaction between SFB and methyldopa was investigated using a UV spectrophotometer to record the spectrum of 4.0 μM of both SFB and methyldopa, individually in phosphate buffer (pH 6.5), and an equimolar mixture of the monomer–template. The spectra were collected over a 200 to 400 nm wavelength range.

Methyldopa electropolymerization at the surface of PGE

The bare PGEs were first washed using a methanol and water mixture to clean the surface from any impurities. Then, they were dried under a nitrogen stream. Next, as working electrodes, the PGEs were connected, and 2 cm of the electrode was dipped in a solution containing phosphate buffer (pH 6.5), SFB (0.01 M), and methyldopa (0.01 M). Then, the solution was purged for 15 min under a nitrogen stream to remove oxygen. *In situ* electropolymerization was carried out by applying 10 voltammetric cycles against an Ag/AgCl electrode from 0.0 V to 0.9 V with a 50 mV s^{-1} scan rate. Then, the polymerized electrodes, denoted as MIP/PGE, were left in the washing solution composed of glacial acetic acid/methanol (2 : 8, v/v) for 20 min under gentle stirring. Finally, the polymerized electrodes were rinsed with water and dried to be used in the next step.

The surface chemical composition of the prepared electrodes was characterized by XPS. The electrochemical characterization was conducted in 0.1 M KCl solution containing an equimolar 5 mM $[Fe(CN)_6]^{3-/4-}$ redox probe using both electrochemical impedance spectroscopy (EIS) and CV.

Electrochemical measurements of SFB

Before the analysis was carried out, the MIP/PGE was immersed for 10 min in the test solution with stirring, and then washed with water for 30 s. A solution of 5.0 mM $[Fe(CN)6]^{3-/4-}$ in the presence of 0.1 M KCl was measured in phosphate buffer (pH 7.0) by differential pulse voltammetry (DPV) within a potential window of −0.2 to 0.8 V *versus* the Ag/AgCl reference electrode at ambient temperature. The calibration curve was constructed by plotting the normalized reduction in the current peak height of redox probe *versus* the corresponding concentration ranging from 1.0×10^{-13} M to 1.0×10^{-11} M SFB.

Application of a pharmaceutical dosage form

Ten tablets, containing 400 mg of SFB, were weighed then entirely crushed into a fine powder. A weighed amount equivalent to 53 mg of SFB of the produced powder was dissolved in 100 mL of phosphate buffer (pH 7.0). Filtration and further dilutions were then performed with phosphate buffer (pH 7.0) to obtain a final concentration of 1.0×10^{-12} M. Then, the electrochemical measurement was carried out as previously mentioned and the regression equation was used to estimate the SFB concentration.

Application to spiked human plasma

Aliquots of human plasma 1.0 mL were spiked with 1.0 mL of 1×10^{-3} M SFB standard solution then mixed ultrasonically for 20 min. Next, the samples were purified by adding 3.5 mL of acetonitrile which precipitated the plasma proteins. Finally, the samples were centrifuged for 20 min at high speed. Several aliquots from the supernatant were then transferred and diluted to 25 mL using a phosphate buffer solution (pH 7.0) to obtain a final concentration of 5.0×10^{-12} M. Electrochemical measurements were then carried out and the average recoveries were calculated.

Method validation

As stated by the International Council for Harmonisation of Technical Requirements for Pharmaceuticals for Human Use (ICH) guidelines, the suggested method was validated in terms of linearity, accuracy, precision, and limits of quantification and detection. The linearity was evaluated under optimum conditions by measuring five SFB concentrations. The plot of the normalized reduction in current peak height *vs.* concentration in range of 1.0×10^{-13} M to 1.0×10^{-11} M gave the linear correlation. The accuracy of the analytical method indicated the closeness between the actual and the reported values, and was expressed as the percentage recovery of the studied drug's various levels in standard solutions. Both intraday (on the same day) and interday (on three different days) precision were evaluated by quantifying three different drug concentrations within the linearity range. Then, the results were expressed as relative standard deviation percentage (% RSD),

and then the limit of quantification (LOQ) and limit of detection (LOD) were also calculated.

Interference

Both structurally similar drugs (entecavir, oseltamivir, tenofovir) and co-administered drugs (ledipasvir) were utilized for studying the selectivity of the sensor, and the ability to quantitively determine SFB in the presence of its interfering drugs. The current peak height change in the presence of interfering ions (1.0×10^{-6} M), which was a million times the concentration of SFB under optimized conditions, was measured.

Results and discussion

Evaluation of the template–monomer interactions by UV-spectrophotometry

Spectrophotometric techniques usually provide rapid, cost-effective and powerful tools to screen different complexes formed between a template and a monomer, and to optimize their stoichiometric ratio.[47–49] So, the investigation of monomers and their possible complexes in phosphate buffer solution was carried out spectrophotometrically at pH 6.5. As shown in Fig. 2, the SFB/methyldopa mixture gave an absorption spectrum with a hypochromic shift, and it was compared to the calculated sum of the SFB/methyldopa spectra that reflected the formation of a complex between SFB and methyldopa.[48,50]

Methyldopa electropolymerization on PGE surface

Using our previous study as guidance,[18] the development and optimization of a novel method was conducted for methyldopa electropolymerization using the CV technique. The PGEs were used for electrochemical measurements as they are feasible, disposable, eco-friendly, cost-effective, and simpler than other conventional carbon electrodes.[51,52] The voltammogram of the electropolymerization of methyldopa when applying voltages ranging from −0.1 V to 0.9 V, with a scan rate of 50 mV s^{-1} for 10 cycles, is shown in Fig. 3. After the first cycle, the anodic current declined rapidly indicating that there was a high rate of electropolymerization. As intramolecular cyclization of methyldopa molecules has been proposed; oxidation and polymerization to form a melanin-like structure, without losing the functional phenolic and carboxylic groups of methyldopa which are responsible for binding with SFB molecule.[53,54] As shown in Fig. 4, the XPS analysis confirmed this proposed scheme. For the next step, the current of the peak was gradually decreased by increasing the number of voltammetric cycles until it had faded after 10 cycles due to the formation of the adherent PMD polymeric film and complete PGE surface insulation.[55,56] The electropolymerization was performed in the presence of SFB as a template to give the SFB/PGEs.

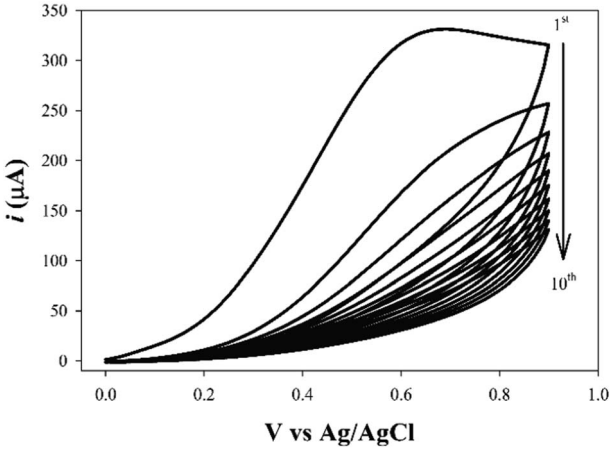

Fig. 3 The cyclic voltammogram of the methyldopa electropolymerization process over 10 cycles.

Characterization of the electropolymerization process

Surface characterization of PGE/MIP. The surface morphology was examined using SEM, and the data are shown

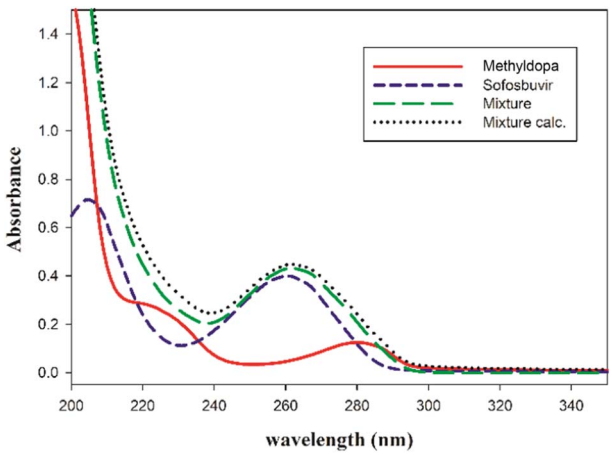

Fig. 2 The UV spectra of the template: sofosbuvir, monomer methyldopa, and the equimolar mixture of both, and the calculated sum of sofosbuvir and methyldopa.

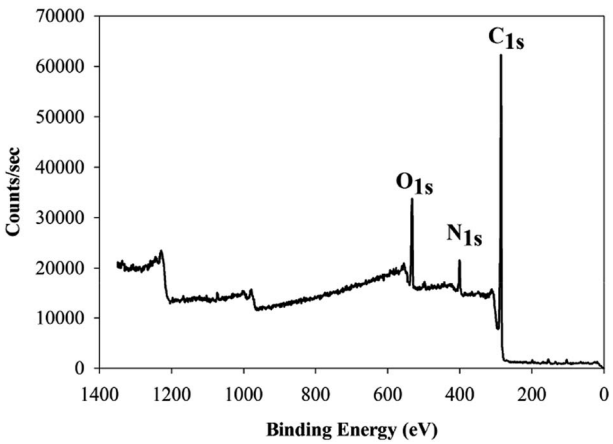

Fig. 4 The X-ray photoelectron survey spectrum of the PGE/PMD modified electrode showing three prominent peaks for C 1s, N 1s, and O 1s.

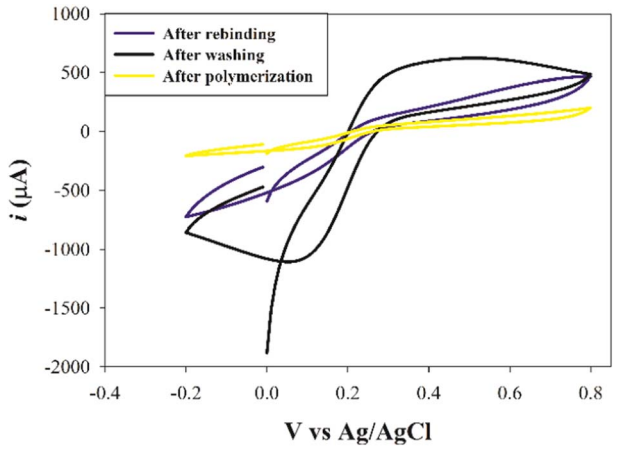

Fig. 5 The cyclic voltammograms of the same electrode for a redox probe solution (equimolar 5 mM $[Fe(CN)_6]^{3-/4-}$ in 0.1 M KCl) after polymerization, after washing, and after rebinding.

in Fig. S1(A) (ESI†), where the images clearly indicate the presence of a uniformly distributed polymer layer onto the PGE surface, indicating the successful electropolymerization of MIP. To further confirm the electropolymerization and the surface composition of this layer, XPS was also performed. The XPS survey spectrum in Fig. 4 shows the strong peaks of: C 1s at about 286 eV, O 1s peak at about 533 eV, and a third peak of about 401 eV for N 1s. The presence of the N 1s peak presented unequivocal evidence of the successful electropolymerization of PMD film onto the PGE electrode. The high resolution spectra were further analyzed to obtain a deeper understanding of the polymer structure, and Fig. S1(B) (ESI†) shows a C 1s high resolution spectrum, where the deconvolution of the peak was performed showing three bands. The deconvoluted bands were about 284.8 eV, 285.4 eV, and 288.6 eV, corresponding to C=C, C–N, and O–C=O bonds, respectively. Fig. S1(C) (ESI†) shows the deconvolution of the high resolution spectrum of the N 1s region, and the devolution shows two deconvoluted bands at 399.7 eV and 400.5 eV, which correspond to R–NH–R and aromatic N atoms, respectively. Fig. S1(D) (ESI†) represents the deconvolution of the high resolution spectrum of the O 1s region, and the two deconvoluted bands at 531.8 eV and 532.7 eV corresponded to the O–C=O and C=O bonds, respectively. These results indicated the successful modification of the surface with the polymer poly(methyldopa) thin layer.

Electrochemical characterization of the PGE/MIP. The CV technique has been widely adopted by many researchers[57–59] to investigate several polymerization stages as shown in Fig. 5, using a ferrocyanide/ferricyanide redox probe. Once the electropolymerization step has been completed, and before template removal, the peak current value at the SFB/PGE surface has been clearly diminished. This reflects the insulation of the whole PGE surface with a film of PMD, and this prevents electron transfer.[57] The redox probe peaks had been retained after washing the PGE with an extraction solvent of glacial acetic acid/methanol (2 : 8, v/v). This observation might be attributed to the removal of the template drug which left cavities in the MIP matrix acting as channels to enable the transfer of the redox probe. Upon rebinding with SFB molecules, a remarkable decrease in the redox probe signal occurred due to the blocking of these channels. Furthermore, these results reflected the ability to produce an imprinted cavity that was able to adsorb the analyte by the elution process.

Moreover, the EIS has been used to study the changes occurring in the electrode surfaces during the process of modification, and the data were fitted to Randle's circuit as shown in Fig. 6. The charge transfer resistance (R_{ct}) for the PGE/MIP sensor, after polymerization and before elution, showed a high R_{ct} (1157 Ω), which decreased after the template removal to a R_{ct} value of 410 Ω and indicated the formation of a binding cavity. Finally, after incubation in the SFB solution, the R_{ct} (916.9 Ω) had increased again, indicating the successful rebinding to the MIP cavities. These results indicated that the R_{ct} after polymerization was high due to the formation of the ultrathin polymer film, whereas the washing resulted in the

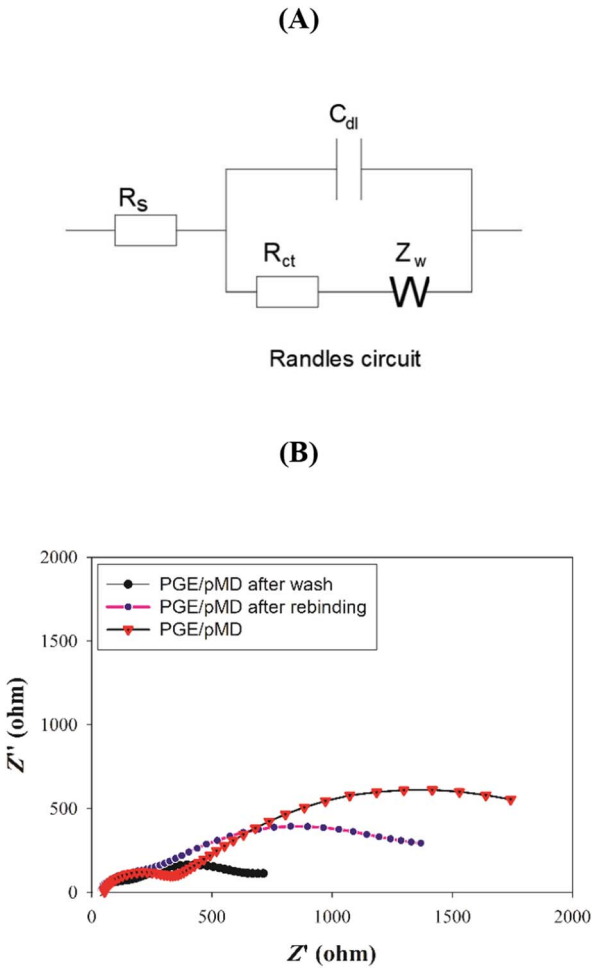

Fig. 6 (A) Randles circuit diagram used for fitting the EIS data. (B) The Nyquist plots of the same electrode during the modification process (after polymerization, after washing, and after rebinding) in the redox probe solution of equimolar 5.0 mM $[Fe(CN)_6]^{3-/4-}$ in the presence of 0.1 M KCl at a frequency range of 100 kHz to 100 mHz.

elution of the drug, and hence, enabled the redox probe to diffuse into the cavities, and thus, the R_{ct} decreased, whereas the rebinding excluded the redox probe and the R_{ct} increased.

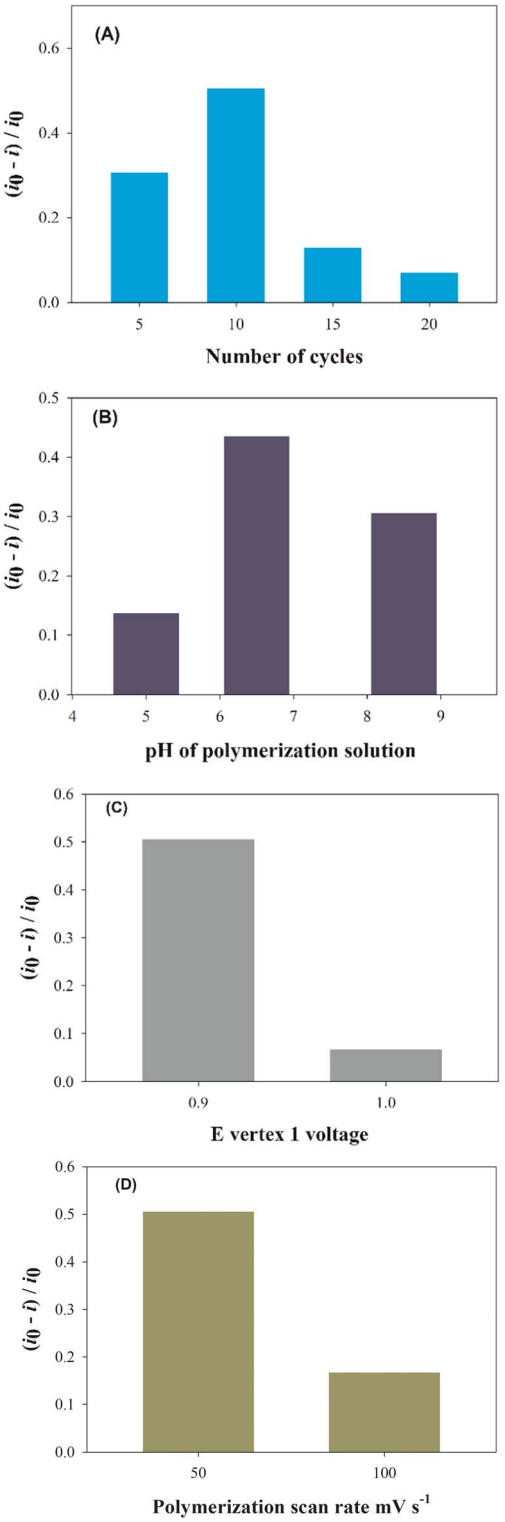

Fig. 7 The optimization of various parameters affecting the electropolymerization process of methyldopa. (A) Number of cycles, (B) electropolymerization pH, (C) *E* vertex 1 voltage, and (D) scan rate.

The results of the measurements of the faradaic impedance showed good agreement with the results of the CV.

Method optimization for methyldopa electropolymerization. The electropolymerization method was optimized for increasing the sensor sensitivity by optimizing the experimental conditions.[9,10,60] Deliberate small changes in the experimental parameters, such as number of cycles, polymerization pH, potential window for electropolymerization, and scan rate, were tested using a univariate optimization study (by changing one variable at a time). Fig. 7 reflects the results obtained for each parameter studied at different levels. Upon increasing the number of cycles to 10, the maximum response was achieved, and then it declined with an increasing number of cycles (Fig. 7A). During polymerization, the pH had an important role in the polymerization behavior. A pH of 6.5 was observed to produce the optimum response (Fig. 7B). Furthermore, the potential window during electropolymerization was another important factor which determined the form of the PMD. It was found that applying a potential window of 0.9 V *vs.* Ag/AgCl had a better response than applying a potential window to 1.0 V as shown in Fig. 7C. The current response had altered by using a different scan rate and the maximum response was found at 50 mV s^{-1} (Fig. 7D). Consequently, the optimization studies allowed a maximized sensor response towards the SFB.

Electrochemical measurement of SFB using SFB/PGEs. The DPV response of the redox probe at the PGE/MIP surface was recorded at various SFB concentrations as shown in Fig. 8. Construction of the calibration curve was carried out by plotting the normalized reduction in the current peak height $((i_0 - i)/i_0)$ *vs.* SFB molar concentration as shown in Fig. 9. The SFB response was linear in the concentration range (1.0×10^{-13} to 1.0×10^{-11} mol L^{-1}) using the modified electrode under optimum conditions. The linear regression equation was $((i_0 - i)/i_0)$ $\mu A = -0.0722x$ (pmol L^{-1}) + 0.9262, and the correlation coefficient was $r = 0.995$. The LOD and LOQ were calculated to be 3.1×10^{-14} mol L^{-1} ($3\sigma/m$) and 9.39×10^{-14} mol L^{-1} ($10\ \sigma/$

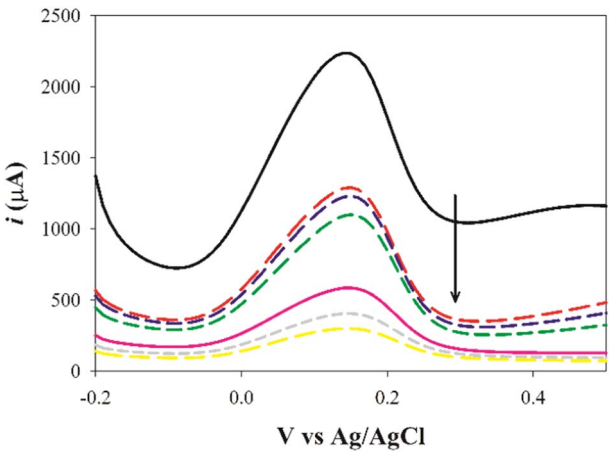

Fig. 8 Differential pulse voltammograms of redox probe (equimolar of 5 mM $[Fe(CN)_6]^{3-/4-}$ in 0.1 M KCl) at MIP/PGE surface in the presence of various concentrations of SFB ranging from 1.0×10^{-13} M to 1.0×10^{-11} M.

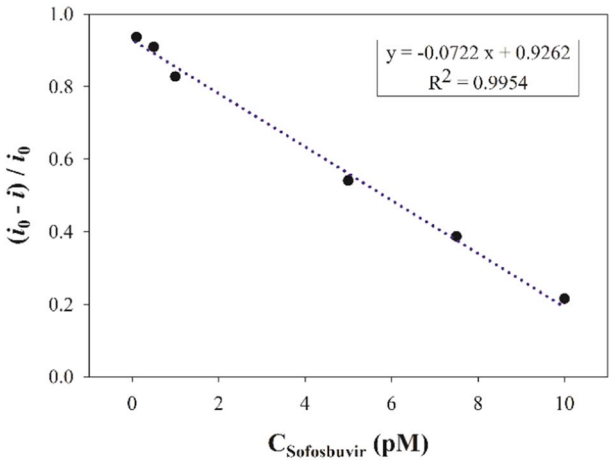

Fig. 9 The calibration curve of SFB solutions ranging from 1.0 × 10^{-13} M to 1.0 × 10^{-11} M at optimum conditions.

m), respectively, where σ is the standard deviation of the blank and m is the slope of the calibration curve.

Analytical performance of the proposed SFB sensor. For the SFB quantitative estimation using SFB/PGEs, we applied a DPV technique instead of CV, because the use of DPV enabled a better signal-to-noise ratio and a higher current sensitivity, where the current was recorded as the difference before applying the pulse and after the decay of the charging current. The method was been observed to be linear within range of 1.0 × 10^{-13} to 1.0 × 10^{-11} M under the optimum electrochemical conditions. The correlation coefficient of the method was 0.995. The results of the linearity are summarized in Table 1 and Fig. 9. Moreover, the suggested method accuracy was proven by the examination of three different levels of SFB and calculation of the percentage recovery. The % RSD values were proved to be within the accepted range which was not more than 2% for the interday and intraday precision. This proved that the proposed method is precise. The results of the LOD, LOQ, accuracy, and the % RSD were calculated and are summarized in Table 1.

Selectivity. The selectivity results are summarized in Table 2. Oseltamivir, ledipasvir, tenofovir, and entecavir were used to investigate the MIP selectivity, where the measured concentration was 1.0 × 10^{-6} mol L^{-1} which represented one millionth of the concentration of SFB. The normalized current peak reductions of the redox probe were shown to be 36.7%, 28.7%, 32.9%, and 48.2% for oseltamivir, ledipasvir, tenofovir, and entecavir, respectively. Consequently, it was concluded that these analogues did not interfere with the DPV detection of SFB, thus showing the high selectivity of the MIP sensor.

Table 1 The proposed electrochemical performance of the sensor based on IUPAC recommendations

Parameter	Sofosbuvir
Slope	−0.0722 pM
Correlation coefficient (r)	0.995
Intercept	0.926
Range of linearity (M)	1.0 × 10^{-11} M to 1.0 × 10^{-13} M
Accuracy (mean ± SD)	102.83 ± 1.45
Precision (% RSD)	
Intraday precision	1.41
Interday precision	1.99
LOD	3.1 × 10^{-14} M
LOQ	9.39 × 10^{-14} M

Table 2 Evaluation of the selectivity of the proposed sensor for SFB in the presence of interfering molecules with one millionth of the concentration of the SFB analyte

Interferant	Concentration	Current reduction (%)
Entecavir	1 × 10^{-6} M	36.7
Ledipasvir	1 × 10^{-6} M	28.7
Tenofovir	1 × 10^{-6} M	32.9
Oseltamivir	1 × 10^{-6} M	48.2

Application in dosage form and spiked plasma samples. The proposed MIP/PGE electrode for use in the quantification of SFB using its pharmaceutical tablet formulation, Nucleobuvir, was developed. Measurements of DPV were done in triplicate, where a suitable average recovery percentage with % RSD did not exceed 2.0, was obtained, as shown in Table 3. These results revealed that the method had a satisfactory recovery, which indicating that the fabricated MIP had high recognition affinity for SFB. For assuring the applicability of the suggested electrochemical MIP sensor for determination of the targeted drug in real samples of pharmaceutical formulation, statistical analyses using the F-test and the Student's t-test were performed to compare the results of the proposed and reported method.[61] The P value was adjusted at 0.05, and the computed Student's t-test and F-test values proved to be less than their relative tabulated ones, which indicated the lack of an evident statistical difference between the suggested and reported methods, and the reliability of the suggested sensor to quantify SFB. Furthermore, the suggested method gave a lower LOD than the reported ones, which indicated that methyldopa has a higher selectivity for SFB. In addition, the proposed method has confirmed the efficacy of methyldopa for MIP film synthesis based on the development of an electropolymerization method. For the spiked plasma samples, the proposed sensor was employed for the measurements of SFB, and the average percentage recovery was calculated to be 97.43% based on three samples with an RSD of 1.38. These results indicated that the

Table 3 Statistical comparison between the reported and the proposed method for the SFB determination in a Nucleobuvir® dosage form

	Nucleobuvir® tablet dosage form	
Parameters	Proposed sensor	Reported method[61]
n	5	5
Mean ± SD	101.14 ± 1.63	100.78 ± 1.68
Variance	2.65	2.78
% RSD	1.61	1.65
t (2.30)	0.34	
F (6.38)	1.05	

Table 4 A comparison between the proposed sensor and some traditional methods for SFB determination

	Range of linearity	Time of response	LOD	LOQ	Ref. no.
Proposed method	1.0×10^{-11} M to 1.0×10^{-13} M	30 s	3.1×10^{-14}	9.39×10^{-14}	—
HPLC	4–48 μg mL^{-1}	7 min	0.015 μg mL^{-1}	0.046 μg mL^{-1}	62
HPLC	160–480 μg mL^{-1}	3.674 min	0.04 μg	0.125 μg	63
HPLC	0.05–0.15 mg mL^{-1}	5 min	0.001 mg mL^{-1}	0.003 mg mL^{-1}	64
Spectrophotometry	0.6–30 μg mL^{-1}	30 s	0.5764 μg mL^{-1}	1.7468 μg mL^{-1}	65
Electrochemical (MIP)	$0.1–40.0 \times 10^{-8}$ M	30 s	0.036×10^{-8} M	1.188×10^{-9} M	41
Electrochemical (MIP)	0.53–74.13 ng mL^{-1}	30 s	0.05 ng mL^{-1}	0.165 ng mL^{-1}	40

proposed PGE/MIP sensor has a great potential for the selective and rapid determination of SFB in real plasma samples. A comparison between the proposed sensor and some traditional methods for SFB determination summerized in Table 4.

Conclusion

In this research, methyldopa has been used as a functional monomer to design a highly selective MIP-based sensor for sofosbuvir analysis. As a functional monomer, methyldopa offers many advantages such as having both phenolic and carboxylic functional groups that permit various interactions with the template molecule. The interaction occurs between methyldopa as a monomer and the template sofosbuvir, and this was studied by UV spectroscopy and results indicated that a complex was formed between them. The electrochemical sensor was fabricated by the electropolymerization of methyldopa at pH 6.5 in the presence of the sofosbuvir. The conditions of the experiment such as pH, number of cycles, polymerization potential window, and scan rate were optimized to enhance the selectivity for the target molecule. The characterization methods employed such as SEM, XPS, CV, and EIS provided conclusive evidence of the formation of poly(methyldopa) on the PGE surface, and the formation of the 3D cavities for sofosbuvir. The proposed sensor showed a high selectivity for PMD–MIP even in the presence of interferents with concentrations 6 orders of magnitude greater than that of the analyte, and indirect detection using a ferrocyanide/ferricyanide redox probe enabled great sensitivity. The MIP sensor is a promising platform for sofosbuvir that is capable of determining sofosbuvir in a pharmaceutical formulation and in spiked human plasma with acceptable recoveries and precision.

Conflicts of interest

There are no conflicts to declare.

References

1 H. Lee, S. M. Dellatore, W. M. Miller and P. B. Messersmith, Mussel-inspired surface chemistry for multifunctional coatings, *Science*, 2007, **318**(5849), 426–430.
2 Z. Jin, L. Yang, S. Shi, T. Wang, G. Duan, X. Liu and Y. Li, Flexible polydopamine bioelectronics, *Adv. Funct. Mater.*, 2021, **31**(30), 2103391.
3 J.-G. Wang, X. Hua, M. Li and Y.-T. Long, Mussel-inspired polydopamine functionalized plasmonic nanocomposites for single-particle catalysis, *ACS Appl. Mater. Interfaces*, 2017, **9**(3), 3016–3023.
4 R. Batul, T. Tamanna, A. Khaliq and A. Yu, Recent progress in the biomedical applications of polydopamine nanostructures, *Biomater. Sci.*, 2017, **5**(7), 1204–1229.
5 W. Cheng, X. Zeng, H. Chen, Z. Li, W. Zeng, L. Mei and Y. Zhao, Versatile polydopamine platforms: synthesis and promising applications for surface modification and advanced nanomedicine, *ACS Nano*, 2019, **13**(8), 8537–8565.
6 T. G. Barclay, H. M. Hegab, S. R. Clarke and M. Ginic-Markovic, Versatile surface modification using polydopamine and related polycatecholamines: chemistry, structure, and applications, *Adv. Mater. Interfaces*, 2017, **4**(19), 1601192.
7 S. Li, H. Wang, M. Young, F. Xu, G. Cheng and H. Cong, Properties of electropolymerized dopamine and its analogues, *Langmuir*, 2018, **35**(5), 1119–1125.
8 H. Guo, Y. Sun, X. Niu, N. Wei, C. Pan, G. Wang, H. Zhang, H. Chen, T. Yi and X. Chen, The preparation of poly-levodopa coated capillary column for capillary electrochromatography enantioseparation, *J. Chromatogr. A*, 2018, **1578**, 91–98.
9 P. T. Pınar, Y. Yardım and Z. Şentürk, Electrochemical oxidation of ranitidine at poly (dopamine) modified carbon paste electrode: its voltammetric determination in pharmaceutical and biological samples based on the enhancement effect of anionic surfactant, *Sens. Actuators, B*, 2018, **273**, 1463–1473.
10 M. Amiri, E. Amali and A. Nematollahzadeh, Poly-dopamine thin film for voltammetric sensing of atenolol, *Sens. Actuators, B*, 2015, **216**, 551–557.
11 W. Lei, Q. Wu, W. Si, Z. Gu, Y. Zhang, J. Deng and Q. Hao, Electrochemical determination of imidacloprid using poly (carbazole)/chemically reduced graphene oxide modified glassy carbon electrode, *Sens. Actuators, B*, 2013, **183**, 102–109.
12 H. Yang, Z. Wei, S. He, T. Li, Y. Zhu, L. Duan, Y. Li and J. Wang, Fabrication of electrochemical sensor for acetaminophen based on levodopa polymer and multi-walled carbon nanotubes complex, *Int. J. Electrochem. Sci.*, 2017, **12**, 11089–11101.
13 P. Supraja, S. Tripathy, S. R. K. Vanjari, V. Singh and S. G. Singh, Electrospun tin (IV) oxide nanofiber based

electrochemical sensor for ultra-sensitive and selective detection of atrazine in water at trace levels, *Biosens. Bioelectron.*, 2019, **141**, 111441.

14 P. Sharma, A. Pietrzyk-Le, F. D'Souza and W. Kutner, Electrochemically synthesized polymers in molecular imprinting for chemical sensing, *Anal. Bioanal. Chem.*, 2012, **402**(10), 3177–3204.

15 G. Liu, J. Zhao, S. Lu, S. Wang, J. Sun and X. Yang, Polymethyldopa nanoparticles-based fluorescent sensor for detection of tyrosinase activity, *ACS Sens.*, 2018, **3**(9), 1855–1862.

16 H. Veisi, S. Hemmati and P. Safarimehr, In situ immobilized palladium nanoparticles on surface of poly-methyldopa coated-magnetic nanoparticles (Fe3O4@ PMDA/Pd): a magnetically recyclable nanocatalyst for cyanation of aryl halides with K4 [Fe (CN) 6], *J. Catal.*, 2018, **365**, 204–212.

17 S. Lotfi and H. Veisi, Pd nanoparticles decorated poly-methyldopa@ GO/Fe3O4 nanocomposite modified glassy carbon electrode as a new electrochemical sensor for simultaneous determination of acetaminophen and phenylephrine, *Mater. Sci. Eng. C*, 2019, **105**, 110112.

18 M. Wadie, E. M. Abdel-Moety, M. R. Rezk, A. M. Mahmoud and H. M. Marzouk, Electro-polymerized poly-methyldopa as a novel synthetic mussel-inspired molecularly imprinted polymeric sensor for darifenacin: computational and experimental study, *Appl. Mater. Today*, 2022, **29**, 101595.

19 L. Chen, X. Wang, W. Lu, X. Wu and J. Li, Molecular imprinting: perspectives and applications, *Chem. Soc. Rev.*, 2016, **45**(8), 2137–2211.

20 M. Wadie, H. M. Marzouk, M. R. Rezk, E. M. Abdel-Moety and M. A. Tantawy, A sensing platform of molecular imprinted polymer-based polyaniline/carbon paste electrodes for simultaneous potentiometric determination of alfuzosin and solifenacin in binary co-formulation and spiked plasma, *Anal. Chim. Acta*, 2022, **1200**, 339599.

21 N. J. Vickers, Animal communication: when i'm calling you, will you answer too?, *Curr. Biol.*, 2017, **27**(14), R713–R715.

22 L. M. Goncalves, Electropolymerized molecularly imprinted polymers: perceptions based on recent literature for soon-to-be world-class scientists, *Curr. Opin. Electrochem.*, 2021, **25**, 100640.

23 M. Naveen, N. Gurudatt and Y. Shim, Applications of conducting polymer composites to electrochemical sensors: a review, *Appl. Mater. Today*, 2017, **9**, 419–433.

24 J. Niu, J. Li and P. Liu, Facile fabrication of flexible, bendable and knittable electrode with PANI in the well-defined porous rEGO/GP fiber for solid state supercapacitors, *Appl. Mater. Today*, 2020, **20**, 100733.

25 S. Motia, B. Bouchikhi, E. Llobet and N. El Bari, Synthesis and characterization of a highly sensitive and selective electrochemical sensor based on molecularly imprinted polymer with gold nanoparticles modified screen-printed electrode for glycerol determination in wastewater, *Talanta*, 2020, **216**, 120953.

26 S. M. Alqahtani, M. A. Alamri, A. Alabbas, P. Alam, S. A. Abdel-Gawad, F. Shakeel and F. A. Alasmary, Spectrophotometric and spectrodensitometric quantification of a new antiviral combination, *J. Planar Chromatogr. - Mod. TLC*, 2020, **33**(1), 79–87.

27 J.-M. Molina, C. Orkin, D. M. Iser, F.-X. Zamora, M. Nelson, C. Stephan, B. Massetto, A. Gaggar, L. Ni and E. Svarovskaia, Sofosbuvir plus ribavirin for treatment of hepatitis C virus in patients co-infected with HIV (PHOTON-2): a multicentre, open-label, non-randomised, phase 3 study, *Lancet*, 2015, **385**(9973), 1098–1106.

28 A. A. Eltahla, F. Luciani, P. A. White, A. R. Lloyd and R. A. Bull, Inhibitors of the hepatitis C virus polymerase; mode of action and resistance, *Viruses*, 2015, **7**(10), 5206–5224.

29 A. Cha and A. Budovich, Sofosbuvir: a new oral once-daily agent for the treatment of hepatitis C virus infection, *Pharm. Ther.*, 2014, **39**(5), 345.

30 E. Cholongitas and G. V. Papatheodoridis, Sofosbuvir: a novel oral agent for chronic hepatitis C, *Ann. Gastroenterol.*, 2014, **27**(4), 331.

31 L. Rose, T. E. Bias, C. B. Mathias, S. B. Trooskin and J. J. Fong, Sofosbuvir: a nucleotide NS5B inhibitor for the treatment of chronic hepatitis C infection, *Ann. Pharmacother.*, 2014, **48**(8), 1019–1029.

32 A. F. El-Yazbi, N. E. Elashkar, H. M. Ahmed, W. Talaat and K. M. Abdel-Hay, Cost-effective green chromatographic method for the simultaneous determination of four commonly used direct-acting antiviral drugs in plasma and various pharmaceutical formulations, *Microchem. J.*, 2021, **168**, 106512.

33 A. Jouyban, M. A. Farajzadeh, F. Khodadadeian, M. Khoubnasabjafari and M. R. A. Mogaddam, Development of a deep eutectic solvent-based ultrasound-assisted homogenous liquid-liquid microextraction method for simultaneous extraction of daclatasvir and sofosbuvir from urine samples, *J. Pharm. Biomed. Anal.*, 2021, **204**, 114254.

34 R. E. Kannouma, M. A. Hammad, A. H. Kamal and F. R. Mansour, A dispersive liquid–liquid microextraction method based on solidification of floating organic droplet for determination of antiviral agents in environmental water using HPLC/UV, *Microchem. J.*, 2021, **171**, 106790.

35 S. Miraghaei, B. Mohammadi, A. Babaei, S. Keshavarz and G. Bahrami, Development and validation of a new HPLC-DAD method for quantification of sofosbuvir in human serum and its comparison with LC–MS/MS technique: application to a bioequivalence study, *J. Chromatogr. B*, 2017, **1063**, 118–122.

36 D. Ferrari, S. Bagaglio, M. Raso, L. Galli, S. Premaschi, E. Messina, G. Morsica, M. Locatelli, C. Uberti-Foppa and H. Hasson, A liquid chromatography-tandem mass spectrometry method for simultaneous determination of simeprevir, daclatasvir, sofosbuvir, and GS-331007 applied to a retrospective clinical pharmacological study, *J. Chromatogr. B*, 2019, **1120**, 1–7.

37 O. M. Abdallah, A. M. Abdel-Megied and A. S. Gouda, Development and validation of LC-MS/MS method for simultaneous determination of sofosbuvir and daclatasvir

in human plasma: application to pharmacokinetic study, *Biomed. Chromatogr.*, 2018, **32**(6), e4186.

38 N. N. Atia, S. R. El-Shaboury, S. M. El-Gizawy and M. N. Abo-Zeid, Simultaneous quantitation of two direct acting hepatitis C antivirals (sofosbuvir and daclatasvir) by an HPLC-UV method designated for their pharmacokinetic study in rabbits, *J. Pharm. Biomed. Anal.*, 2018, **158**, 88–93.

39 A. F. El-Yazbi, Comparative validation of the determination of sofosbuvir in pharmaceuticals by several inexpensive ecofriendly chromatographic, electrophoretic, and spectrophotometric methods, *J. AOAC Int.*, 2017, **100**(4), 1000–1007.

40 M. A. H. A. Tawab, M. G. Abd El-Moghny and R. M. El Nashar, Computational design of molecularly imprinted polymer for electrochemical sensing and stability indicating study of sofosbuvir, *Microchem. J.*, 2020, **158**, 105180.

41 A. M. Mahmoud, M. M. El-Wekil, M. H. Mahnashi, M. F. Ali and S. A. Alkahtani, Modification of N, S co-doped graphene quantum dots with p-aminothiophenol-functionalized gold nanoparticles for molecular imprint-based voltammetric determination of the antiviral drug sofosbuvir, *Microchim. Acta*, 2019, **186**, 1–8.

42 A. Abdallah, A. El-Shafei and M. E. Khalifa, Selective and sensitive electrochemical sensor based on molecular imprinting strategy for recognition and quantification of sofosbuvir in real samples, *Arabian J. Sci. Eng.*, 2021, 1–11.

43 D. Elfadil, A. Lamaoui, F. Della Pelle, A. Amine and D. Compagnone, Molecularly imprinted polymers combined with electrochemical sensors for food contaminants analysis, *Molecules*, 2021, **26**(15), 4607.

44 A. Herrera-Chacón, X. Cetó and M. Del Valle, Molecularly imprinted polymers-towards electrochemical sensors and electronic tongues, *Anal. Bioanal. Chem.*, 2021, **413**, 6117–6140.

45 N. F. Atta, A. Galal and Y. M. Ahmed, New strategy for determination of anti-viral drugs based on highly conductive layered composite of MnO2/graphene/ionic liquid crystal/carbon nanotubes, *J. Electroanal. Chem.*, 2019, **838**, 107–118.

46 N. F. Atta, A. Galal and Y. M. Ahmed, Electrochemical method for the determination of three new anti-hepatitis C drugs: application in human blood serum, *J. Electrochem. Soc.*, 2018, **165**(10), B442.

47 K. Karim, F. Breton, R. Rouillon, E. V. Piletska, A. Guerreiro, I. Chianella and S. A. Piletsky, How to find effective functional monomers for effective molecularly imprinted polymers?, *Adv. Drug Delivery Rev.*, 2005, **57**(12), 1795–1808.

48 M. Zhang, H. Zhao, T. Xie, X. Yang, A. Dong, H. Zhang, J. Wang and Z. Wang, Molecularly imprinted polymer on graphene surface for selective and sensitive electrochemical sensing imidacloprid, *Sens. Actuators, B*, 2017, **252**, 991–1002.

49 M. K. Abd El-Rahman, G. Mazzone, A. M. Mahmoud, E. Sicilia and T. Shoeib, Novel choline selective electrochemical membrane sensor with application in milk powders and infant formulas, *Talanta*, 2021, **221**, 121409.

50 S. A. Fahmy, F. Ponte, I. M. Fawzy, E. Sicilia, U. Bakowsky and H. M. E.-S. Azzazy, Host-Guest Complexation of Oxaliplatin and Para-Sulfonatocalix [n] Arenes for Potential Use in Cancer Therapy, *Molecules*, 2020, **25**(24), 5926.

51 S. Sharma, R. Jain and A. N. Raja, Pencil graphite electrode: an emerging sensing material, *J. Electrochem. Soc.*, 2020, **167**(3), 037501.

52 H. Z. Yamani, N. Safwat, A. M. Mahmoud, M. F. Ayad, M. F. Abdel-Ghany and M. M. Gomaa, Point-of-care diagnostics for rapid determination of prostate cancer biomarker sarcosine: application of disposable potentiometric sensor based on oxide-conductive polymer nanocomposite, *Anal. Bioanal. Chem.*, 2023, 1–12.

53 J. Cai, J. Huang, M. Ge, J. Iocozzia, Z. Lin, K. Q. Zhang and Y. Lai, Immobilization of Pt nanoparticles via rapid and reusable electropolymerization of dopamine on TiO2 nanotube arrays for reversible SERS substrates and nonenzymatic glucose sensors, *Small*, 2017, **13**(19), 1604240.

54 N. Leibl, L. Duma, C. Gonzato and K. Haupt, Polydopamine-based molecularly imprinted thin films for electro-chemical sensing of nitro-explosives in aqueous solutions, *Bioelectrochemistry*, 2020, **135**, 107541.

55 J. C. Zuaznabar-Gardona and A. Fragoso, Development of highly sensitive IgA immunosensors based on co-electropolymerized L-DOPA/dopamine carbon nano-onion modified electrodes, *Biosens. Bioelectron.*, 2019, **141**, 111357.

56 H. M. El-Sayed, H. E. Abdellatef, A. M. Mahmoud, H. A. Hendawy, O. M. El-Abassy and H. Ibrahim, Safinamide detection based on Prussian blue analogue modified Solid-contact potentiometric sensor, *Microchem. J.*, 2023, **191**, 108829.

57 A. Cetinkaya, S. I. Kaya, G. Ozcelikay, E. B. Atici and S. A. Ozkan, A molecularly imprinted electrochemical sensor based on highly selective and an ultra-trace assay of anti-cancer drug axitinib in its dosage form and biological samples, *Talanta*, 2021, **233**, 122569.

58 N. Karimian, A. P. Turner and A. Tiwari, Electrochemical evaluation of troponin T imprinted polymer receptor, *Biosens. Bioelectron.*, 2014, **59**, 160–165.

59 K. Kor and K. Zarei, Development and characterization of an electrochemical sensor for furosemide detection based on electropolymerized molecularly imprinted polymer, *Talanta*, 2016, **146**, 181–187.

60 N. F. El Azab, A. M. Mahmoud and Y. A. Trabik, Point-of-care diagnostics for therapeutic monitoring of levofloxacin in human plasma utilizing electrochemical sensor mussel-inspired molecularly imprinted copolymer, *J. Electroanal. Chem.*, 2022, **918**, 116504.

61 N. Karimian, A. M. Stortini, L. M. Moretto, C. Costantino, S. Bogialli and P. Ugo, Electrochemosensor for trace analysis of perfluorooctanesulfonate in water based on a molecularly imprinted poly (o-phenylenediamine) polymer, *ACS Sens.*, 2018, **3**(7), 1291–1298.

62 B. Zaman and W. Hassan, Development of Stability Indicating HPLC-UV Method for Determination of Process Impurities and Degradation Products in Sofosbuvir and Velpatasvir Tablets, *Pharm. Chem. J.*, 2021, **54**, 1295–1305.

63 S. Ganji, S. Dhulipala and A. R. Nemala, Development and validation of RP HPLC method for the estimation of Sofosbuvir and related impurity in bulk and pharmaceutical dosage form, *Future J. Pharm. Sci.*, 2021, **7**, 1–10.
64 G. R. Mangrio, A. Maneengam, Z. Khalid, T. H. Jafar, G. Q. Chanihoon, R. Nassani and A. Unar, RP-HPLC method development, validation, and drug repurposing of sofosbuvir pharmaceutical dosage form: a multidimensional study, *Environ. Res.*, 2022, **212**, 113282.
65 B. A. Bhairav and M. J. Chavan, Method Development and Validation to Estimate Sofosbuvir in Marketed preparation by UV-Spectroscopy and HPLC along with force Degradation Study, *Res. J. Pharm. Technol.*, 2021, **14**(8), 4165–4172.